

MSG SEVIRI APPLICATIONS FOR WEATHER AND CLIMATE: CLOUD PROPERTIES AND CALIBRATIONS

Patrick Minnis⁽¹⁾, Louis Nguyen⁽¹⁾, William L. Smith⁽¹⁾, Rabindra Palikonda⁽²⁾, David R. Doelling⁽²⁾
J. Kirk Ayers⁽²⁾, Qing Z. Trepte⁽³⁾, Fu-Lung Chang⁽⁴⁾

⁽¹⁾NASA Langley Research Center, MS 420, Hampton, VA 23681 USA, Email: p.minnis@nasa.gov

⁽²⁾AS&M, Inc., 1 Enterprise Parkway, Hampton, VA 23666 USA, Email: d.r.doelling@larc.nasa.gov

⁽³⁾SAIC, 1 Enterprise Parkway, Hampton, VA 23666 USA, Email: q.z.trepte@larc.nasa.gov

⁽⁴⁾National Institute of Aerospace, 100 Exploration Way, Hampton, VA 23666 USA, Email: fchang@nianet.org

ABSTRACT

SEVIRI data are cross-calibrated against the corresponding *Aqua* and *Terra* MODIS channels. Compared to *Terra* MODIS, no significant trends are evident in the 0.65, 0.86, and 1.6 μm channel gains between May 2004 and May 2006, indicating excellent stability in the solar-channel sensors. On average, the corresponding *Terra* reflectances are 12, 14, and 1% greater than the their SEVIRI counterparts. The *Terra* 3.8- μm channel brightness temperatures T are 7 and 4 K greater than their SEVIRI counterparts during day and night, respectively. The average differences between T for MODIS and SEVIRI 8.6, 10.8, 12.0, and 13.3- μm channels are between 0.5 and 2 K. The cloud properties are being derived hourly over Europe and, in initial comparisons, agree well with surface observations. Errors caused by residual calibration uncertainties, terminator conditions, and inaccurate temperature and humidity profiles are still problematic. Future versions will address those errors and the effects of multilayered clouds.

1. INTRODUCTION

The Meteosat Second Generation (MSG) 3-km resolution Spin-Enhanced Visible Infrared Imager (SEVIRI) provides the opportunity to monitor weather systems throughout the diurnal cycle with unprecedented temporal and spatial resolution using a combination of spectral channels heretofore available only on lower Earth-orbiting (LEO) satellites. For the past 7 years, a set of algorithms has been applied to data from high-resolution LEO satellite imagers for the Clouds and Earth's Radiant Energy System (CERES) Project [1] and from the 4-km resolution, 5-channel Geostationary Operational Environmental Satellite (GOES) imager over the United States (US) [2]. The CERES algorithms use up to 8 channels on the 32-channel Moderate Resolution Imaging Spectroradiometer (MODIS) on *Aqua* and *Terra*, but only 4 channels from GOES. The upcoming generation of GOES, the GOES-R series, will be more like the SEVIRI than its predecessors. Thus, to determine how well the CERES algorithms work on geostationary satellites using more than 4 channels to help prepare for

the use of the future GOES-R, to evaluate the algorithms over a full range of conditions, and to develop algorithm improvements, among other objectives, this MSG RAO effort has been designed to apply the CERES algorithms to SEVIRI data and evaluate and refine the results. To obtain consistency with retrievals from the other satellites, it is necessary to ensure that the satellites are properly intercalibrated. Previous studies presented initial intercalibrations [3] and cloud retrievals over a European domain [4] results from early MSG data. Progress in improving the calibrations and retrievals has continued and is reported here. The retrievals are currently being performed over a European domain each hour. To validate the retrievals, results over the Chilbolton, UK and Cabauw, Netherlands, surface sites are compared with similar quantities derived from active and passive sensors.

2. DATA

The calibrations are performed using *Meteosat-8* SEVIRI and *Terra* and *Aqua* MODIS data taken from April 2004 through May 2006. The SEVIRI (MODIS) channels of interest are the visible (VIS) 0.64 (0.64) μm , 0.80 (0.86) μm , near-infrared (NIR) 1.62 (1.62) μm , the solar-infrared (SIR) 3.9 (3.8) μm , 8.7 (8.6) μm , infrared (IR) 11.0 (10.8) μm , split-window (SWC) 12.0 (12.0) μm , and CO_2 13.3 (13.3) μm bands. An additional comparison is performed using the GOES-12 SIR channel. The satellite detection and retrieval of single-layer cloud properties use the VIS, NIR, SIR, IR, and SWC channels. Multilayered cloud retrievals also use the CO_2 channel. Efforts to utilize the 8.7- μm channel are underway. Data from the European domain, extending from 30°N to 55°N and from 12°W to 30°E, are analyzed each hour at 6-km resolution obtained by sampling every other pixel and scan line. The Western Europe domain (39°N - 54°N; 4°W - 17°E) is analyzed at the 3-km resolution for better comparisons with ground site data. The data are analyzed in near-real time, but display is delayed for 24 hours. The auxiliary data needed for analysis include temperature, humidity and ozone profiles from the 6-hourly 1.25° NOAA Global Forecast System (GFS) analyses. Other input datasets are described by [4].

3. METHODOLOGY

3.1. Calibration

The calibrations were performed following the methods of [5] and [6]. Collocated and matched *Terra* MODIS and SEVIRI pixels taken over ocean were averaged to 0.5° regions using a 30° x 20° grid box near the M8 sub-satellite point. The data matched if the differences Δx in solar zenith, viewing zenith, and relative azimuth angles and time meet the following criteria:

$$\Delta SZA < 15^\circ, \Delta VZA < 10^\circ, \Delta RAZ < 15^\circ, \Delta t < 15\text{min},$$

respectively. No data taken in sunglint are used. For the purposes of intercalibrating, it is assumed that the corresponding MODIS and SEVIRI channels have the same filter function. The time differences are taken in to account using the ratios of $\cos(SZA)$. Spectral differences were not taken into account in the intercalibrations.

When a one month of data have been acquired, the SEVIRI solar channels are calibrated in terms of the MODIS radiance,

$$L_M = a [C(M8) - C_o(M8)] F_o(M) / F_o(M8) \quad (1)$$

where a is the gain, C is the observed 10-bit count, C_o is the space count, F_o is the spectral solar constant, M refers to MODIS, and $M8$ refers to SEVIRI. For all channels with wavelengths exceeding 2.0 μm , the radiances are fit in terms of the brightness temperatures,

$$T_M = b T_{M8} + b_o, \quad (2)$$

where b is the slope and b_o is the offset. The mean differences, $T_{M8} - T_M$, are also computed each month to measure trends in SEVIRI channels because trends in the slopes can offset by opposite trends in the offsets.

3.2. Cloud Properties

Cloudy pixels are detected with a version of the CERES Cloud Mask [1, 2, 4] and the corresponding cloud properties are retrieved using the suite of CERES cloud property retrieval algorithms that include the VIS-IR-SIR-SWC Technique (VISST) during the daytime, the SIR-IR-SWC Technique (SIST) at night [7], and the SIR-IR-NIR Technique [8] during the day over snow-covered surfaces. The retrievals use a consistent set of models characterizing water droplet and hexagonal ice column reflectances and emittances [9] within a set of parameterizations [10]. The resulting output for each pixel in every image includes many different parameters, such as latitude (LAT) and longitude (LON), that are summarized in Tab. 1. The results for each image are stored digitally and used to create images of each parameter for the specific domain. These images as well as the archived data can be accessed via the Internet at <http://www-angler.larc.nasa.gov/satimage/products.html>. At that web page, the data for

Table 1. VISST output parameters for each pixel

LAT, LON, SZA, VZA, RAZ
Scene ID (Clear or Phase)
Clear-sky effective temperature
Cloud effective temperature
Cloud effective height and pressure
Cloud top height
Cloud thickness (base height)
Cloud emissivity
Cloud water droplet effective radius or ice effective diameter
Cloud optical depth
Cloud liquid water or ice water path
Broadband SW albedo & LW flux
Aircraft icing index
Reflectance or temperature at 0.64, 3.9, 10.8, 12.0, 13.3 μm

the European domain can be accessed through the link, “EUROPE”. Figure 1 shows an example of the “EUROPE” web page for image time 0900 UTC, 13 June 2006. The RGB image is displayed for the most recent analysis that is available. Links to the Western Europe domain and to averaged properties for five different ground sites in Europe are provided on the page. The images for any parameter at any time when data were analyzed can be displayed using a pull-down menu that allows control of the parameter, number of images, and starting. Either one or four variables can be displayed and looped. Archived digital data and other satellite cloud products can be accessed via links listed on the page.

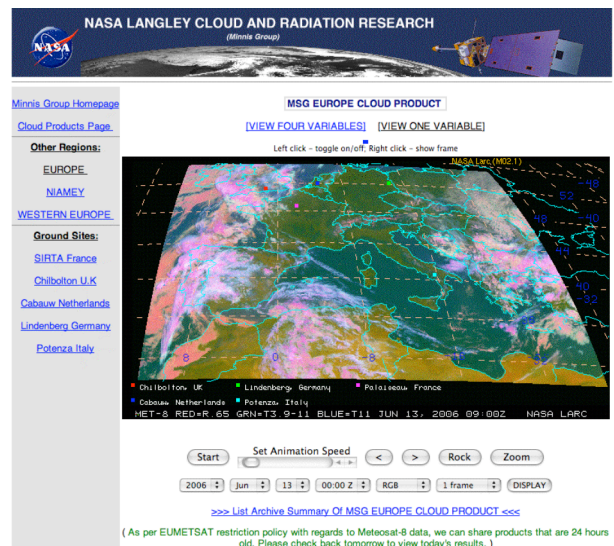


Figure 1. Example of European domain web page accessed via “EUROPE” link.

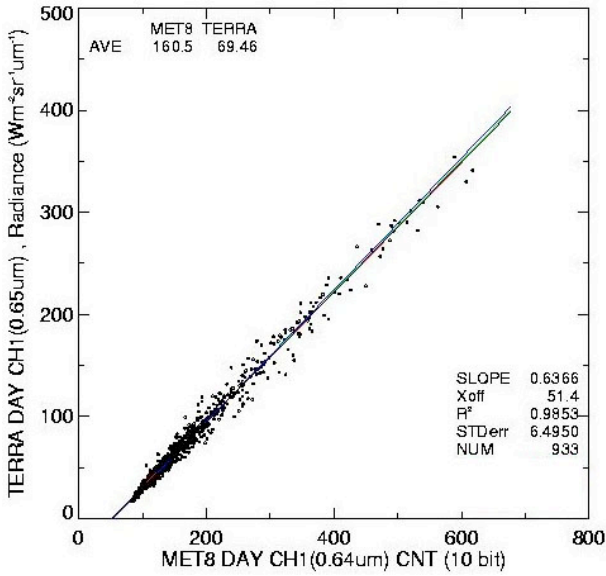


Figure 2. Terra MODIS radiance as function of SEVIRI VIS count, November 2005.

4. RESULTS

4.1. Calibrations

Fig. 2 shows the scatterplot and linear regression fit using the Terra VIS channel during November 2005. The scatter is relatively minor, except at the brighter end of the range. The resulting slope and offset are 0.6366 and 51.4, respectively. The offset is very close to the nominal space count of 51.0. Similar plots and fits were made for each month during the period for all of the solar channels and used to estimate the trends in the gains and offsets. The mean slopes are listed in Tab. 2 along with the mean gains provided operationally by EUMETSAT. The result in Fig. 2 is typical for the VIS channels. The mean gain from *Terra* is $0.639 \text{ Wm}^{-2} \text{ sr}^{-1} \mu\text{m}^{-1}$, a value that is 11% greater than the operational value. The mean offset count is 52.1. The respective results from *Aqua* are nearly identical at $0.637 \text{ Wm}^{-2} \text{ sr}^{-1} \mu\text{m}^{-1}$ and 52.5. No statistically significant trend was found in either set of gains. Based on radiative transfer calculations, it is expected that the MODIS reflectance should be only 2.1% greater than the SEVIRI value for a given ocean scene. Given that MODIS has an onboard calibration system, these results suggest that the SEVIRI VIS channels could be too dark by 9%. This corrected VIS calibration is used in the cloud retrievals.

Table 2. Mean gains in SEVIRI solar channels from EUMETSAT and Terra, May 2004 – May 2006.

Channel μm	EUMETSAT $\text{Wm}^{-2} \text{ sr}^{-1} \mu\text{m}^{-1}$	<i>Terra</i> $\text{Wm}^{-2} \text{ sr}^{-1} \mu\text{m}^{-1}$	Difference (%)
0.64	0.573	0.639	11.5
0.80	0.453	0.518	14.3
1.62	0.088	0.089	1.1

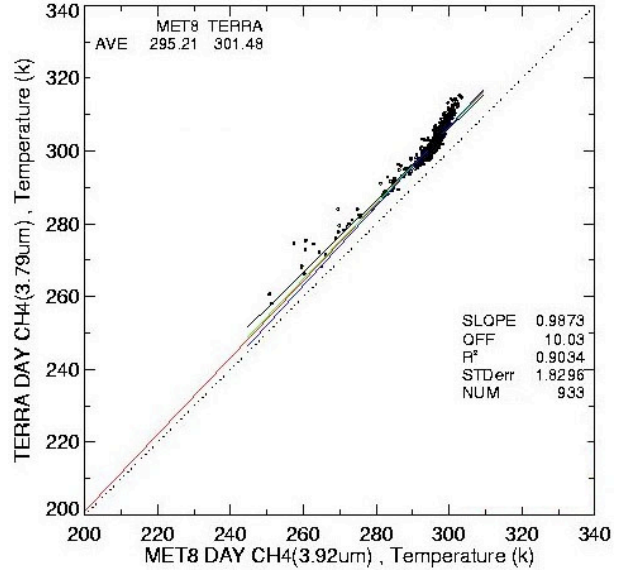


Figure 3. Terra MODIS SIR temperature as function of SEVIRI SIR temperature, daytime, November 2005.

No trends were found in any of the other solar channels. However, the MODIS $0.86\text{-}\mu\text{m}$ reflectance averages 14.3% more than the SEVIRI $0.81\text{-}\mu\text{m}$ reflectance (Tab. 2). That difference may be entirely due to spectral differences and will require additional study to determine if it is significant. The mean offset is 52.9. The differences in the NIR channel are negligible. The SEVIRI band is considerably wider than the MODIS channel, but both are symmetrically centered on the same wavelength. The mean NIR offset is 51.3 counts.

Fig. 3 shows the November 2005 daytime correlation of the SIR channels, which indicates that the MODIS temperatures are 6 K greater, on average. The result is quite typical as indicated in Tab. 3. At night, the relationship changes and the difference between the two channels decreases. Comparisons with the GOES-12 channel (not shown) yields the same results during both day and night; the GOES temperatures average 3.1 K greater than their SEVIRI counterparts. Good agreement is found at $T < 260 \text{ K}$ in both instances. Differences in the other channels are much smaller, as indicated in Tab. 3, especially for the IR and SWC channels. The SEVIRI CO_2 channel is much broader than for MODIS.

Table 3. Linear fits and differences between SEVIRI and Terra brightness temperatures, May 2004 – May 2006.

Channel (μm)	Slope	Offset	Diff (K)
3.90 (day)	1.125	-30.1	-6.67
3.90 (night)	1.041	-8.02	-3.73
8.60	0.982	5.74	-0.45
10.8	1.008	3.09	0.70
12.0	1.010	3.28	0.45
13.3	0.955	10.5	1.52

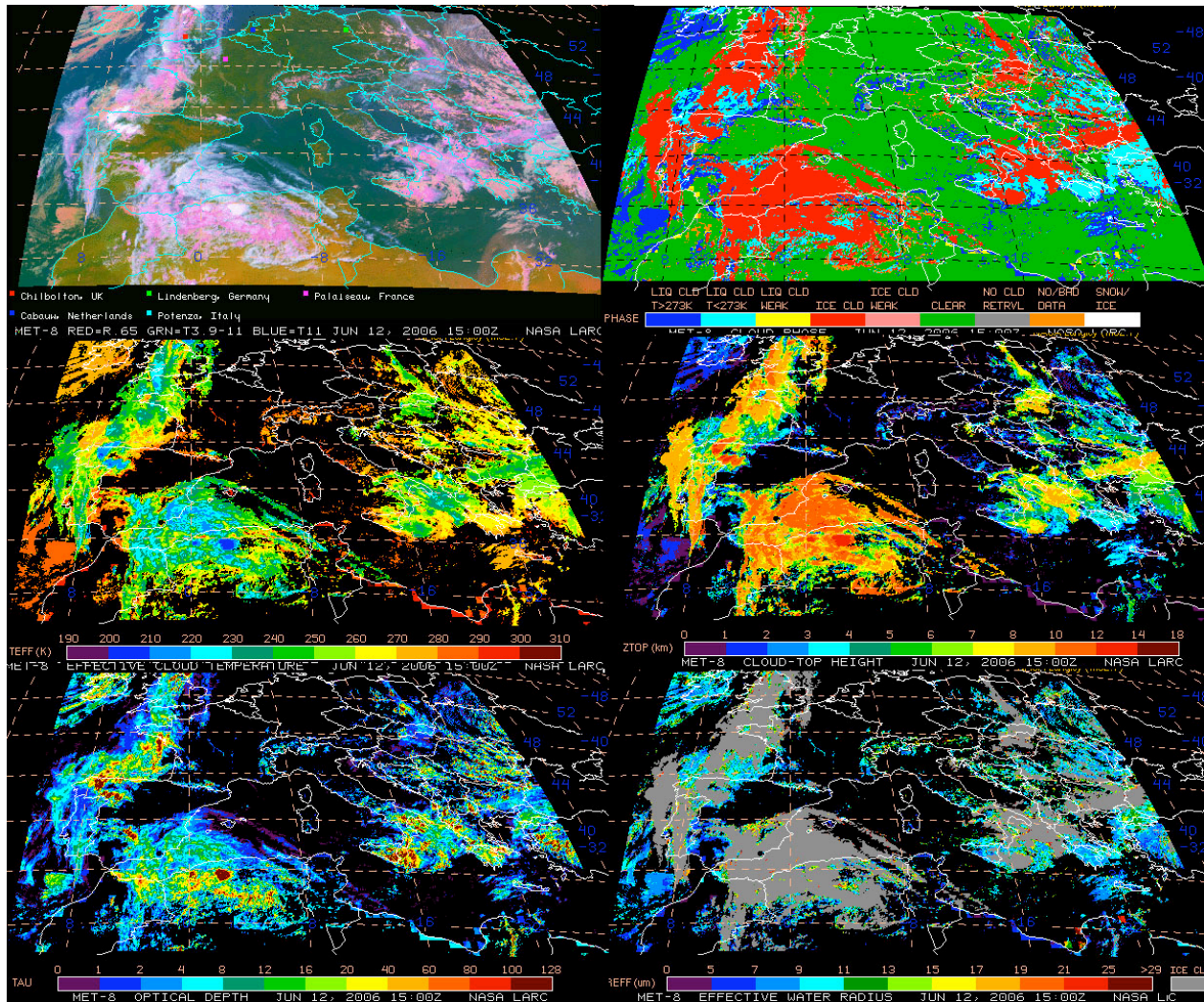


Figure 4. Example of products from cloud retrieval, 1500 UTC, 12 June 2006. Clockwise from top right: RGB image, phase, cloud-top height, water droplet effective radius, cloud optical depth, and cloud effective temperature.

4.2 Satellite Products & Access

Examples of several product images are shown in Fig. 4 for 1500 UTC, 12 June 2006. A frontal system with ice clouds on top is passing over the British, French, and Iberian coasts, while cirrus and other ice clouds indicate a low pressure system over Algeria. Cloud top heights reach up to 14 km over Algeria. The effective droplet sizes are generally between 9 and 11 μm except for some smaller values off the Moroccan coast and north of Libya. The greatest optical depths are seen over Algeria, southern Italy, and northwestern Spain. Clouds with tops between 1 and 2 km cover Ireland. These results are fairly typical. Some of the thinner clouds are not detected and a few false clouds are generated along the north African coasts. In some instances, a given 0.5° box is classified as a clear whenever the GFS temperature profiles are in error or the clear-sky temperatures or albedo are not properly characterized. Other errors are produced whenever the SZA is between 85 and 90° because the SIR signal is insufficient.

4.2 Validation

The cloud products can be assessed visually by examining images of the results and the radiances together. That approach yields a qualitative evaluation that identifies many gross errors. Comparisons with objective measurements from the surface or from aircraft is more valuable for obtaining a quantitative verification of the results. The initial evaluations [4] used data taken at the SIRTa site in Palaiseau, France and from automated surface observing systems across Europe. Here, the active and passive sensors at Chilbolton, UK and Cabauw, Netherlands are used to assess a few of those parameters at those sites, which are indicated on the RGB image in Fig. 4. The Cabauw cloud radar is used in preliminary manner to assess the cloud boundaries, while the Chilbolton ceilometer is used to assess cloud base for single-layer clouds and the LWP derived from the microwave radiometer is compared to the same parameter derived from SEVIRI using VISST.

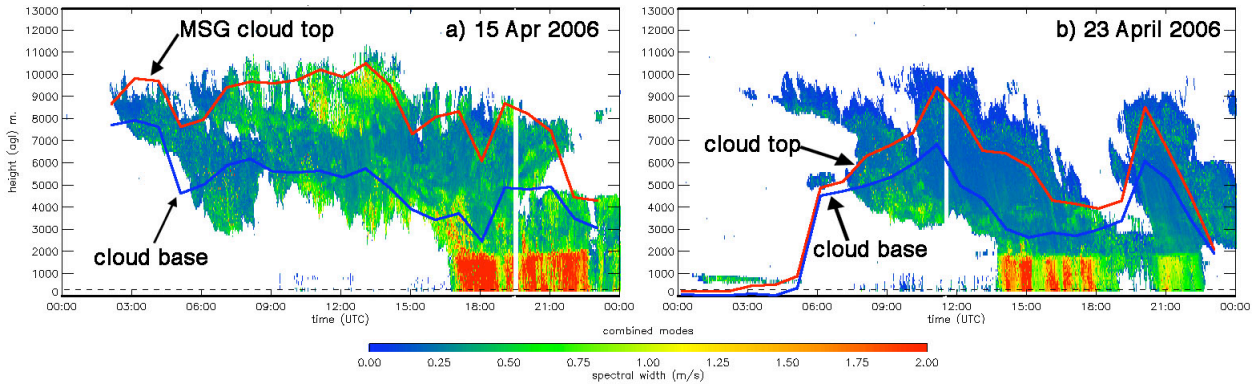


Figure 5. Cloud boundaries at Cabauw, Netherlands from cloud radar and Meteosat-8 using VISST and SIST.

Cloud boundaries from the VISST/SIST analyses track the cirrus boundaries determined from the Cabauw cloud radar during 15 April 2006 (Fig. 5a). Precipitation falls out below the cloud bases. The agreement is not as close during 23 April 2006 (Fig. 5b) when the thin low clouds are missed between 0100 and 0200 UTC and the cloud physical thickness is much greater than inferred by the satellite parameterization. Other images (not shown) have revealed the terminator problems noted earlier and some errors due to the temperature profiles.

Fig. 6 shows compares cloud-base heights for single-layer clouds derived from the Chilbolton lidar during daytime in February 2006. The satellite values, averages for a circle with a radius of 20 km centered on the site, are compared to 1-h lidar averages. The mean difference is only 0.1 km, while the RMS differences is 0.82. The comparisons for 3 months are summarized in Tab. 4. Overall, the satellite retrieval overestimates cloud-base height by 240 m with an RMS difference of 1 km. This result is fairly typical for single-layer clouds analyzed with the VISST.

The cloud LWP was derived from the surface microwave radiometer for the same months and compared to the VISST retrievals for single-layer clouds. The scatterplot and statistics are shown in Fig. 7.

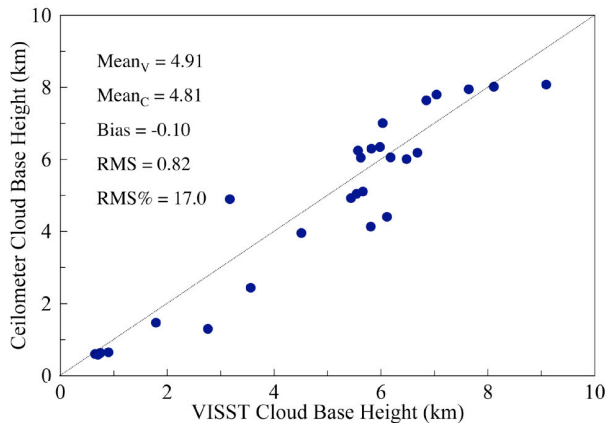


Figure 6. VISST-derived cloud base compared to Chilbolton lidar cloud base, February 2006.

Table 3. Lidar cloud base heights and differences with VISST retrievals over Chilbolton, UK, 2006.

Month	Sfc ht (km)	Diff (km)	RMS (km)	RMS (%)	N
Jan	1.34	-0.37	0.65	49	34
Feb	4.81	-0.10	0.82	17	28
Mar	4.94	-0.37	1.29	26	33
Total	3.61	-0.24	0.97	27	95

The average difference is less than 1%, however, the instant differences can be much larger as indicated by the scatter and the RMS error of 63%. This scatter is somewhat larger than seen in surface-satellite comparisons and could be due to greater variability in the surface data or using less than optimal averaging times and areas.

5. CONCLUDING REMARKS

The intercalibrations between SEVIRI and MODIS are encouraging. SEVIRI appears to have very stable solar channels with relatively good absolute calibrations. The procedures discussed here will be applied to future SEVIRI data to develop a long time record. Spectral differences will be taken into account to determine the actual corrections that should be applied to the data.

While the cloud properties often appear to be quite reasonable, much additional work is needed. Areas for improvement include the terminator, thin cirrus, and

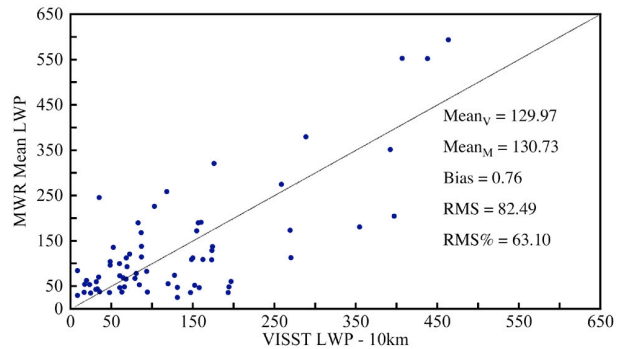


Figure 7. Same as Fig. 6, but for LWP, Jan-Mar 2006.

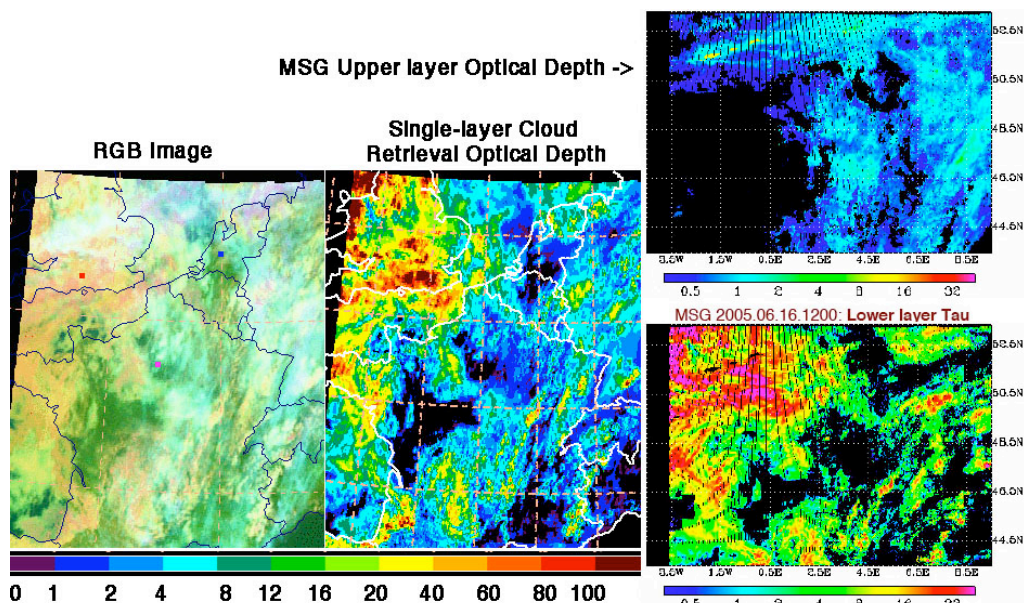


Figure 8. Example of multilayered cloud retrieval from SEVIRI data over Western Europe, 16 June 2006.

multilayered clouds. Efforts to address multilayered cloud retrievals have begun with the use of the method of [11] using the CO₂ channel. The example in Fig. 8 shows that the technique can separate the low and high clouds quite reasonably. This approach and others will be used to address the current shortcomings.

6. ACKNOWLEDGMENTS

This research was supported by the NASA Science Mission Radiation Sciences Branch and the NOAA GOES-R program. The MODIS data were obtained from the NASA Langley Research Center Atmospheric Sciences Data Center and the SEVIRI and GOES-12 data are from the University of Wisconsin-Madison Space Science and Engineering Center. Special thanks to the Radiocommunications Research Unit at the Rutherford Appleton Laboratory for data taken at Chilbolton, UK and to KNMI for the Cabauw radar data.

7. REFERENCES

1. Minnis P., et al. Real-time cloud, radiation, and aircraft icing parameters from GOES over the USA, *Proc. 13th AMS Conf. Satellite Oceanogr. and Meteorol.*, Norfolk, VA, Sept. 20-24, P7.1, 2004.
2. Minnis P., et al. Near real-time satellite cloud products for nowcasting applications. *Proc. WWRP Symp. Nowcasting & Very Short Range Forecasting*, Toulouse, FR, 5-9 Sept., 4.19, 2005.
3. Doelling D. R., P. Minnis, and L. Nguyen, Calibration comparisons between SEVIRI, MODIS, and GOES data. *Proc. MSG RAO Workshop*, Salzburg, Austria, 10-11 September, 149-154, 2004.
4. Minnis P., et al., Comparison of cloud properties from Meteosat-8 and surface observations. *Proc.*

MSG RAO Workshop, Salzburg, Austria, 10-11 September, 91-96, 2004.

5. Minnis P., et al. Rapid calibration of operational and research meteorological satellite imagers, Part II: Comparison of infrared channels. *J. Atmos. Oceanic Technol.*, **19**, 1250-1266, 2002.
6. Minnis P., et al. Rapid calibration of operational and research meteorological satellite imagers, Part I: Evaluation of research satellite visible channels as references. *J. Atmos. Oceanic Technol.*, **19**, 1233-1249, 2002.
7. Minnis P., et al. Cloud Optical Property Retrieval (Subsystem 4.3), "Clouds and the Earth's Radiant Energy System (CERES) Algorithm Theoretical Basis Document, Volume III: Cloud Optical Property Retrieval (Subsystem 4.3)", *NASA RP 1376 Vol. III*, edited by CERES Science Team, pp. 135-176, 1995.
8. Minnis, P., et al. Parameterization of reflectance and effective emittance for satellite remote sensing of cloud properties, *J. Atmos. Sci.*, **55**, 3313-3339, 1998.
9. Platnick S., et al. A solar reflectance method for retrieving cloud optical thickness and droplet size over snow and ice surfaces. *J. Geophys. Res.*, **106**, 15185-15199, 2001.
10. Arduini R. F., P. Minnis, and D. F. Young, Investigation of a visible reflectance parameterization for determining cloud properties in multilayered clouds, *Proc. 11th AMS Conf. Cloud Physics*, Ogden, UT, June 3-7, CD-ROM, P2.4, 2002.
11. Chang F.-L. and Z. Li, A new method for detection of cirrus overlapping water clouds and determination of their optical properties, *J. Atmos. Sci.*, **62**, 3993-4009, 2005.